Scalar Dark Matter in the Inert Doublet and Singlet Model with Vectorlike Quarks

The 32nd Vietnam School of Physics (VSOP-32)
ICISE, Quy Nhon Nam, Gia Lai, Vietnam

Nguyen Minh Hien

Faculty of Physics and Engineering Physics
University of Science, VNU-HCM

Supervised by Assoc. Prof. Dr. Dao Thi Nhung

Student Seminar ▪ July 2026

TRƯỜNG ĐẠI HỌC KHOA HỌC TỰ NHIÊN
KHTN
ĐHQG-HCM

HCMUS
Viet Nam National University
Ho Chi Minh City
University of Science

FULL THEORETICAL AND PHENOMENOLOGICAL ANALYSIS

Dark matter constitutes a substantial fraction of the energy density of the Universe, yet its microscopic nature remains unknown. The Standard Model does not contain a viable particle candidate with the required stability, abundance, and interaction strength, which motivates extensions involving new fields protected by a discrete symmetry. Among the simplest possibilities are the real scalar singlet model and the inert doublet model. Both frameworks can provide stable scalar dark matter, but their phenomenology is controlled by a limited set of mechanisms. In the real singlet model, annihilation and direct detection are mainly governed by the Higgs portal, so the same interaction that is needed to obtain an efficient thermal annihilation rate is also restricted by dark-matter searches. In the inert doublet model, electroweak gauge interactions provide additional annihilation channels, but the observed relic abundance is typically obtained in characteristic dynamical regimes, including the Higgs-funnel region and a heavy, nearly degenerate region in which gauge annihilation and coannihilation become important. These minimal models are not necessarily excluded; rather, their viable thermal phenomenology is concentrated in particular parts of parameter space. This motivates the investigation of a framework with additional physical mechanisms that can control dark-matter annihilation and direct detection.

The model considered here extends the Standard Model by an inert scalar doublet, a real scalar singlet, and a doublet of vectorlike quarks. An exact Z2 symmetry separates the visible and dark sectors. All Standard Model fields, including the Standard Model Higgs doublet, are even under Z2, whereas the inert doublet, the real singlet, and the vectorlike-quark doublet are odd. Electroweak symmetry breaking occurs only through the Standard Model Higgs doublet. The inert doublet and the real singlet do not acquire vacuum expectation values, so the Z2 symmetry remains exact after electroweak symmetry breaking. Consequently, the lightest Z2-odd particle cannot decay entirely into Standard Model particles. If this lightest odd particle is electrically neutral, it is stable and can serve as a dark-matter candidate.

The scalar potential contains three quadratic mass parameters, eight quartic couplings, and one dimensionful triple coupling. All parameters are taken to be real, so the scalar sector conserves CP. The electroweak minimum condition, or tadpole equation, is used to eliminate the quadratic parameter associated with the Standard Model Higgs doublet. The measured mass of the Standard Model-like Higgs boson, approximately 125 GeV, then fixes the corresponding Higgs quartic coupling. The remaining parameters determine the masses and interactions of the Z2-odd scalar states. The potential must be bounded from below, the electroweak vacuum must be a consistent minimum, an unwanted charge-breaking vacuum must be avoided, and the scalar interactions must satisfy perturbative unitarity.

The neutral CP-even dark sector contains the real singlet field and the neutral CP-even component of the inert doublet. The dimensionful triple interaction generates an off-diagonal mass term after electroweak symmetry breaking, causing these two fields to mix. Diagonalization produces two physical CP-even states, denoted HD1 and HD2, ordered such that HD1 is lighter than HD2. The state HD1 is chosen to be lighter than the other neutral Z2-odd scalar and is identified as the dark-matter candidate. Its composition is controlled by the mixing angle alpha. For alpha close to zero, HD1 is predominantly singlet-like and has suppressed electroweak interactions. As the magnitude of alpha increases, its doublet component becomes more important, strengthening its interactions with gauge bosons, the Higgs sector, and the vectorlike-quark sector. The mixing angle therefore acts as a physical control parameter for the dark-matter composition, but it does not make the relic abundance and direct-detection rate completely independent because the same underlying couplings can affect several observables.

The vectorlike-quark field is an electroweak doublet with hypercharge seven over six. Both its left-handed and right-handed components transform in the same way under the Standard Model gauge group, which allows a gauge-invariant vectorlike mass term before electroweak symmetry breaking. The upper component, denoted X, has electric charge five thirds and is an exotic quark. The lower component, denoted T, has electric charge two thirds and is therefore top-like in the sense of its electric charge and gauge quantum numbers. The vectorlike-quark doublet is also odd under Z2 and interacts with the inert scalar doublet and right-handed up-type quarks through a Yukawa coupling. The real singlet cannot enter this interaction directly because it does not carry the electroweak doublet index required by gauge invariance. Nevertheless, the singlet influences the vectorlike-quark portal indirectly because the physical dark-matter state is a mixture of singlet and doublet components.

After scalar mixing, the effective interaction between HD1, the top-like vectorlike quark, and an up-type quark is proportional to the vectorlike-quark Yukawa coupling multiplied by the doublet component of HD1. The interaction opens additional annihilation channels into Standard Model fermions through t-channel and u-channel vectorlike-quark exchange. It also produces an additional contribution to elastic dark-matter scattering from quarks. Increasing the Yukawa coupling generally strengthens the quark portal, whereas increasing the vectorlike-quark mass suppresses the amplitudes mediated by the heavy fermion. These two parameters therefore provide additional control, but this freedom has a price: a heavier vectorlike quark is easier to reconcile with collider searches but weakens the portal, while restoring a sizable effect may require a larger Yukawa coupling and can create tension with perturbativity.

The thermal relic abundance is determined by the evolution of the dark-matter number density in the expanding Universe. At high temperatures, dark-matter particles remain in thermal equilibrium with the Standard Model plasma. As the Universe cools, the equilibrium number density decreases and the interaction rate eventually becomes smaller than the expansion rate. Dark matter then freezes out, leaving a relic abundance that survives to the present epoch. The relevant quantity is the thermally averaged effective annihilation rate, which includes all annihilation and coannihilation processes. A larger effective annihilation rate removes more dark-matter particles before freeze-out and therefore produces a smaller relic abundance. Coannihilation becomes important when another Z2-odd particle is sufficiently close in mass to the dark-matter state. If the mass splitting is large compared with the freeze-out temperature, the equilibrium abundance of the heavier state is Boltzmann suppressed and its coannihilation contribution becomes negligible.

The relic abundance must not be confused with the direct-detection cross section. Relic density is controlled by number-changing reactions such as dark-matter annihilation into Standard Model particles, whereas direct detection involves elastic scattering of a dark-matter particle from a quark or nucleon. Elastic scattering does not change the number of dark-matter particles and therefore does not directly enter the Boltzmann equation for the relic abundance. The two observables are nevertheless correlated because they can depend on the same couplings. The same Higgs and vectorlike-quark interactions that generate elastic scattering also generate crossed annihilation processes, but the two reactions occur in different kinematic regimes and their amplitudes need not exhibit the same interference pattern.

At leading tree level, spin-independent dark-matter scattering receives a Standard Model-like Higgs-exchange contribution and a vectorlike-quark-exchange contribution. These contributions must be added at the amplitude level before the cross section is calculated. If the amplitudes have the same sign, the scattering rate can be enhanced. If they have opposite signs and comparable magnitudes, they interfere destructively and the total scattering amplitude can become very small. The resulting suppression produces a direct-detection blind spot. This cancellation is not automatically realized throughout the model and generally occurs only in particular regions of parameter space. Moreover, the vectorlike-quark contribution acts primarily on up-type quarks, whereas the Higgs contribution also remains for down-type quarks and through the effective nucleon matrix elements. The cancellation can therefore be very strong without necessarily being exactly complete at the nucleon level. Loop corrections and other subleading effects may also become relatively important when the leading tree-level amplitude is highly suppressed.

A parameter point is accepted only after several classes of conditions are imposed. The scalar sector must satisfy vacuum stability, the absence of an unwanted charge-breaking vacuum, and tree-level unitarity. The predicted scalar spectrum and Higgs observables must be compatible with searches for additional Higgs bosons and with measurements of the observed 125 GeV Higgs signal. The dark-matter relic abundance is obtained from all relevant tree-level two-to-two annihilation and coannihilation processes, and the spin-independent dark-matter-nucleon cross section is compared with the upper limit from the LUX-ZEPLIN experiment. In the general scan, underabundant dark-matter points can be retained by rescaling the predicted direct-detection rate according to the fraction of the observed dark-matter abundance provided by HD1. Exact-relic points form a more restrictive subset for which HD1 reproduces the observed abundance of approximately 0.120.

An illustrative benchmark has a dark-matter mass of 93 GeV and a mixing angle of approximately 0.543. With the adopted mixing convention, HD1 is mainly singlet-like but contains a non-negligible doublet component. The other Z2-odd scalar states are substantially heavier: the second CP-even scalar has a mass of 329 GeV, the charged scalar has a mass of approximately 321 GeV, and the CP-odd scalar has a mass of approximately 796 GeV. Their thermal abundances at freeze-out are therefore strongly Boltzmann suppressed, so the benchmark relic density is dominated by dark-matter annihilation rather than coannihilation. The calculated relic abundance is approximately 0.120. The predicted spin-independent dark-matter-nucleon cross section is approximately 1.2 times ten to the minus fifty square centimeters, below the LUX-ZEPLIN upper limit quoted in the analysis for a dark-matter mass of 93 GeV. This benchmark demonstrates that the implemented dark-matter and Higgs requirements can be satisfied simultaneously, but it is an illustrative point rather than proof that all possible experimental constraints have been passed.

One-dimensional scans around the benchmark show a strong dependence on the vectorlike-quark Yukawa coupling and the mixing angle. When the Yukawa coupling is varied while the remaining parameters are fixed, the relic abundance is approximately symmetric under a change in the sign of the coupling because the dominant rates depend mainly on even powers of it. The direct-detection cross section develops two sharp, approximately symmetric dips. They correspond to the same cancellation condition at positive and negative Yukawa coupling, since the vectorlike-quark contribution depends primarily on the square of that coupling. The relic-density curve can remain smooth at the same locations because the cancellation is specific to the elastic-scattering amplitude at very small momentum transfer. The thermal relic abundance instead depends on the sum of many annihilation and possible coannihilation channels evaluated in freeze-out kinematics. A cancellation in direct detection therefore does not imply a cancellation of the total annihilation rate.

The scan over the mixing angle exhibits additional structure. Changes in alpha modify the singlet-doublet composition of the dark-matter state and therefore alter its scalar, electroweak, and vectorlike-quark interactions simultaneously. Sharp peaks in the relic abundance indicate regions where the total effective annihilation rate becomes strongly suppressed; they should not automatically be interpreted as particle resonances. Direct-detection dips again indicate destructive interference in the elastic-scattering amplitude. The two sides of the alpha scan need not be exactly symmetric because some scalar interactions contain terms that change sign under alpha changing sign. Only narrow intervals reproduce the observed relic abundance and satisfy the direct-detection requirement when all other parameters are held fixed. These curves are one-dimensional slices through a much larger multidimensional parameter space and must not be interpreted as the complete viable region.

A broader scan reveals exact-relic solutions with dark-matter masses extending approximately from 100 GeV to 1000 GeV under the constraints implemented in the analysis. More surviving points are found above approximately 300 GeV, whereas the lower-mass region is more restricted. The normalized trilinear coupling between two dark-matter particles and the Standard Model-like Higgs is concentrated in a relatively narrow interval around zero. This behavior reflects the need to suppress the Higgs-mediated direct-detection contribution or balance it against the vectorlike-quark contribution. The separated bands in the mixing angle demonstrate that the surviving parameter space is structured rather than uniform. The scan supports the conclusion that singlet-doublet mixing and the vectorlike-quark portal can provide additional mechanisms beyond those of the minimal scalar models, but the density of scan points must not be interpreted as a probability distribution without specifying the scanning measure and prior assumptions.

The additional freedom of the model is not free. A larger parameter space reduces predictivity and can hide correlations among observables. A deep direct-detection blind spot may require a tuned relation between the Higgs and vectorlike-quark amplitudes, as suggested by the narrow cancellation dips. The new scalar and fermionic electroweak doublets contribute to precision observables and require an analysis of the oblique parameters S, T, and U. The colored vectorlike quarks can be produced at hadron colliders, so direct searches for the exotic X and top-like T states, together with their decay topologies and branching ratios, can impose strong constraints. The benchmark and scan discussed here do not constitute a complete collider validation. The vectorlike-quark spectrum must also permit the odd colored states to decay into a Standard Model quark and a lighter Z2-odd scalar; otherwise an unacceptable stable colored particle could result.

Within its stated scope, the analysis establishes several points. The exact Z2 symmetry stabilizes the lightest mixed CP-even scalar and provides a dark-matter candidate. The mixing angle controls the singlet-doublet composition and hence the strength of scalar and electroweak interactions. The vectorlike-quark doublet introduces an additional quark portal that affects annihilation and elastic scattering. Higgs and vectorlike-quark exchange can interfere destructively in direct detection, allowing the spin-independent cross section to be strongly suppressed without requiring the total thermal annihilation rate to vanish. Exact-relic solutions are found over an approximate dark-matter mass range from 100 GeV to 1000 GeV under the implemented theoretical, Higgs, relic-density, and direct-detection requirements. The appropriate conclusion is therefore not that the minimal models fail or that every scanned point is fully viable, but that the combined singlet-doublet and vectorlike-quark framework provides additional physical control over dark-matter phenomenology and motivates a more complete investigation including electroweak precision tests and direct collider constraints.

Do not worry—I will not explain every line.

Motivation

- The real scalar singlet model is strongly constrained by relic-density and direct-detection limits Ref. [1].
- The inert doublet model mainly favors the Higgs-funnel and heavy nearly degenerate regions Ref. [2].
  $\Rightarrow$ Can singlet–doublet mixing and VLQ save the day?

Can the interplay of singlet–doublet mixing and vectorlike-quark interactions yield viable scalar dark matter while satisfying relic-density, Higgs, and direct-detection constraints?

Ref. [3]

Field content and the stabilizing $\mathbb{Z}_2$

Field	$SU(3)_C$	$SU(2)_L$	$U(1)_Y$	$\mathbb{Z}_2$
SM Higgs Φ_1	$\mathbf{1}$	$\mathbf{2}$	$1/2$	$+$
Inert doublet Φ_2	$\mathbf{1}$	$\mathbf{2}$	$1/2$	$-$
Real singlet S	$\mathbf{1}$	$\mathbf{1}$	0	$-$
VLQ doublet $Q_{L/R}$	$\mathbf{3}$	$\mathbf{2}$	$7/6$	$-$

Vacuum configuration

$$\langle \Phi_1 \rangle = \frac{1}{\sqrt{2}} \begin{pmatrix} 0 \\ v \end{pmatrix}, \qquad \langle \Phi_2 \rangle = \langle S \rangle = 0.$$

Consequence

- The $\mathbb{Z}_2$ symmetry remains exact.
- The lightest odd neutral particle is stable.

Scalar Potential

$$
\begin{aligned}
V_H = {} & m_{11}^2 \Phi_1^\dagger \Phi_1 + m_{22}^2 \Phi_2^\dagger \Phi_2 + \frac{\lambda_1}{2} (\Phi_1^\dagger \Phi_1)^2 + \frac{\lambda_2}{2} (\Phi_2^\dagger \Phi_2)^2 \\
& + \lambda_3 (\Phi_1^\dagger \Phi_1)(\Phi_2^\dagger \Phi_2) + \lambda_4 (\Phi_1^\dagger \Phi_2)(\Phi_2^\dagger \Phi_1) \\
& + \frac{\lambda_5}{2} \left[(\Phi_1^\dagger \Phi_2)^2 + \text{h.c.} \right] + \frac{m_S^2}{2} S^2 + \frac{\lambda_6}{8} S^4 \\
& + \frac{\lambda_7}{2} (\Phi_1^\dagger \Phi_1) S^2 + \frac{\lambda_8}{2} (\Phi_2^\dagger \Phi_2) S^2 + \frac{\kappa_{12}}{2} \left[(\Phi_1^\dagger \Phi_2) S + \text{h.c.} \right] .
\end{aligned}
$$

In this study, we choose 11 input parameters: the seven quartic couplings $\lambda_{2,3,4,5,6,7,8}$, the three scalar masses $M_{H_{\rm SM}}, M_{H_{D1}}, M_{H_{D2}}$, and the mixing angle α.

Scalar Mixing Produces the Dark-Matter State

With

$$\Phi_2 = \begin{pmatrix} H^+ \\ (\rho + iA)/\sqrt{2} \end{pmatrix}, \qquad S = \rho_S,$$

the CP-even odd-sector mass matrix in the basis (ρ_S, ρ) is

$$\mathcal{M}^2 = \begin{pmatrix} m_S^2 + \frac{1}{2}\lambda_7 v^2 & \frac{1}{2}\kappa_{12} v \\ \frac{1}{2}\kappa_{12} v & m_{22}^2 + \frac{1}{2}\lambda_{345} v^2 \end{pmatrix}, \lambda_{345} = \lambda_3 + \lambda_4 + \lambda_5.$$

$$\begin{pmatrix} H_{D1} \\ H_{D2} \end{pmatrix} = \begin{pmatrix} \cos\alpha & \sin\alpha \\ -\sin\alpha & \cos\alpha \end{pmatrix} \begin{pmatrix} \rho_S \\ \rho \end{pmatrix}.$$

Choice in this analysis

H_{D1} is taken to be the lightest
$\to$ DM candidate.

$\alpha \simeq 0$: **singlet-like DM** $\qquad$ $|\alpha| \simeq \pi/2$: **doublet-like DM**

▸ Mass-relation derivation

The VLQ is an electroweak doublet, not a singlet

$$Q_{L/R} = \begin{pmatrix} X \\ T \end{pmatrix}_{L/R} \sim (\mathbf{3}, \mathbf{2}, 7/6),$$

$$Q_X = \frac{5}{3}, \qquad Q_T = \frac{2}{3}.$$

The relevant interaction is

$$\mathcal{L}_{\rm VLQ} = -Y_{\rm VLQ}\, \overline{Q}_L \Phi_2^\dagger u_R - m_{\rm VLQ} \overline{Q}_L Q_R + \text{h.c.}$$

Phenomenological role

- t/u-channel VLQ exchange opens $H_{D1} H_{D1} \to u\bar{u}$.
- $Y_{\rm VLQ}$ controls the quark-portal strength.
- $m_{\rm VLQ}$ suppresses both annihilation and scattering amplitudes.

Why Can the VLQ Suppress Direct Detection?

Higgs-mediated scattering

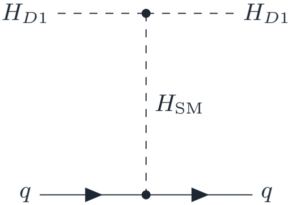

$$\mathcal{M}_h \propto \lambda_{H_{D1}H_{D1}H_{\rm SM}}.$$

VLQ-mediated scattering

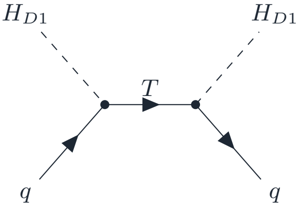

$$\mathcal{M}_T \propto \frac{Y_{\rm VLQ}^2 \sin^2\alpha}{m_{\rm VLQ}^2}.$$

Destructive interference between the Higgs- and VLQ-mediated amplitudes can strongly suppress the spin-independent cross section.

▸ Cancellation condition

What Makes a Parameter Point Acceptable?

Theory

- Vacuum stability
- No charge-breaking vacuum
- Tree-level unitarity

Higgs data

- Additional Higgs searches
- Higgs signal measurements
- Higgs decay constraints

Ref. [11, 12]

Dark matter

- Relic abundance [6]
- Direct detection
- LUX–ZEPLIN limit [7]

A point is retained only if it satisfies all constraints included in the analysis.

From Annihilation to the Relic Density

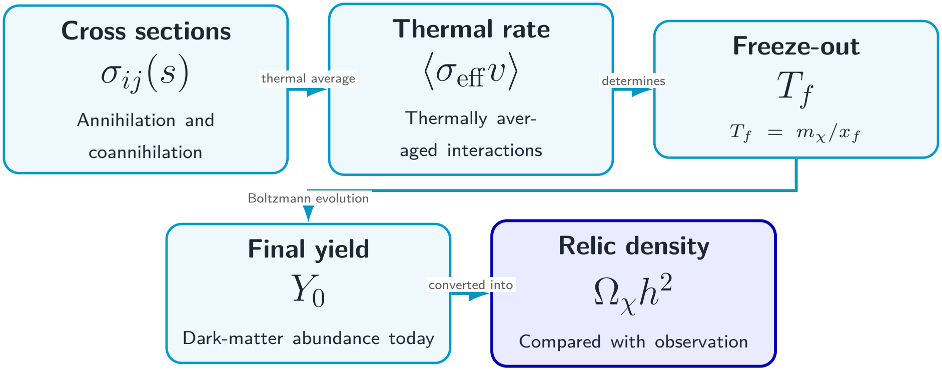

Larger $\langle \sigma_{\text{eff}} v \rangle \implies$ fewer particles after freeze-out $\implies$ smaller $\Omega_\chi h^2$.

An Illustrative Benchmark Point

Benchmark features

- Dark-matter mass:
$$M_{D1} = 93 \text{ GeV}$$
- Singlet–doublet mixing angle:
$$\alpha = 0.543$$
- The other Z_2-odd states are sufficiently heavier than the dark-matter candidate; therefore, coannihilation is negligible.

This benchmark describes a mixed singlet–doublet dark-matter candidate without relevant coannihilation effects.

Source: Dao and Nguyen, PIAS proceeding (2026).

Relic Density Scans

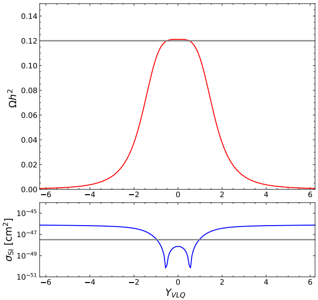

$Y_{\rm VLQ}$ **scan**

The approximate symmetry follows from the even-power dependence on $Y_{\rm VLQ}$.

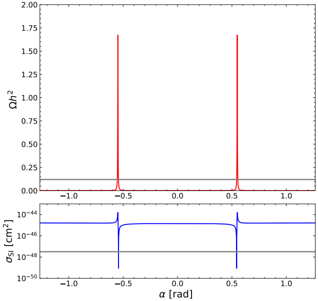

α **scan**

The peaks indicate strongly suppressed annihilation rates.

Only narrow regions reproduce $\Omega_{\rm DM}h^2 \simeq 0.120$.

Source: Dao and Nguyen, PIAS proceeding (2026).

Exact-relic solutions extend across a broad mass range

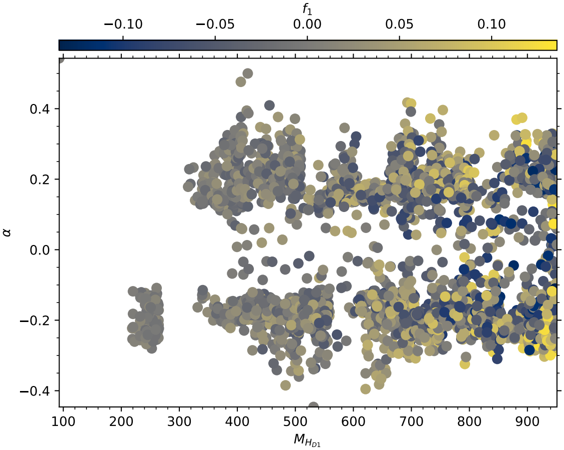

Source: Dao and Nguyen, PIAS proceeding (2026).

- Exact-relic points are found for approximately

$$100\ \mathrm{GeV} \lesssim M_{D1} \lesssim 1000\ \mathrm{GeV}.$$

- More surviving points occur above about 300 GeV.
- The color encodes

$$f_1 = \lambda_{H_{D1}H_{D1}H_{\mathrm{SM}}}/v,$$

generally within a narrow interval around zero.

Results and scope

Main results

- Viable mixed-scalar dark matter is found.
- Relic density, Higgs data, and direct detection are imposed simultaneously.
- Scalar and VLQ contributions can interfere in direct detection.
- Exact-relic points are found for $M_{\mathrm{DM}} \sim 100\text{–}1000\ \mathrm{GeV}$.

Not included

- Electroweak precision constraints: S, T, U
- Direct collider limits on X and T
- Detailed collider signatures

The viable region may change when electroweak-precision and collider constraints are included.

References I

- M. Gonçalves, M. Mühlleitner, R. Santos, and T. Trindade, *Dark Matter in Multi-Singlet Extensions of the Standard Model*, JHEP **03**, 157 (2026), arXiv:2505.07753 [hep-ph].
- A. Belyaev, G. Cacciapaglia, I. P. Ivanov, F. Rojas-Abatte, and M. Thomas, *Anatomy of the Inert Two-Higgs-Doublet Model in the Light of the LHC and Non-LHC Dark Matter Searches*, Phys. Rev. D **97**, 035011 (2018), arXiv:1612.00511 [hep-ph].
- T. N. Dao and M. H. Nguyen, *Scalar Dark Matter in the Inert Doublet and Singlet Model with Vectorlike Quarks*, PIAS proceeding, unpublished (2026).
- D. Azevedo, P. M. Ferreira, M. Mühlleitner, S. Patel, R. Santos, and J. Wittbrodt, *CP in the Dark*, JHEP **11**, 091 (2018), arXiv:1807.10322 [hep-ph].
- F. del Aguila, M. Pérez-Victoria, and J. Santiago, *Observable Contributions of New Exotic Quarks to Quark Mixing*, JHEP **09**, 011 (2000), arXiv:hep-ph/0007316.
- N. Aghanim et al. (Planck Collaboration), *Planck 2018 Results. VI. Cosmological Parameters*, Astron. Astrophys. **641**, A6 (2020), arXiv:1807.06209 [astro-ph.CO].
- J. Aalbers et al. (LUX-ZEPLIN Collaboration), *Dark Matter Search Results from 4.2 Tonne-Years of Exposure of the LUX-ZEPLIN (LZ) Experiment*, Phys. Rev. Lett. **135**, 011802 (2025).
- P. Gondolo and G. Gelmini, *Cosmic Abundances of Stable Particles: Improved Analysis*, Nucl. Phys. B **360**, 145–179 (1991).

References II

- J. Edsjö and P. Gondolo, *Neutralino Relic Density Including Coannihilations*, Phys. Rev. D **56**, 1879–1894 (1997), arXiv:hep-ph/9704361.
- T. Bringmann, J. Edsjö, P. Gondolo, P. Ullio, and L. Bergström, *DarkSUSY 6: An Advanced Tool to Compute Dark Matter Properties Numerically*, JCAP **07**, 033 (2018), arXiv:1802.03399 [hep-ph].
- P. Bechtle et al., *HiggsBounds-5: Testing Higgs Sectors in the LHC 13 TeV Era*, Eur. Phys. J. C **80**, 1211 (2020), arXiv:2006.06007 [hep-ph].
- P. Bechtle, S. Heinemeyer, T. Klingl, T. Stefaniak, G. Weiglein, and J. Wittbrodt, *HiggsSignals-2: Probing New Physics with Precision Higgs Measurements in the LHC 13 TeV Era*, Eur. Phys. J. C **81**, 145 (2021), arXiv:2012.09197 [hep-ph].
- I. Engeln, M. Mühlleitner, and J. Wittbrodt, *N2HDECAY: Higgs Boson Decays in the Different Phases of the N2HDM*, Comput. Phys. Commun. **234**, 256–262 (2019), arXiv:1805.00966 [hep-ph].
- T. Hahn, *Generating Feynman Diagrams and Amplitudes with FeynArts 3*, Comput. Phys. Commun. **140**, 418–431 (2001), arXiv:hep-ph/0012260.
- V. Shtabovenko, R. Mertig, and F. Orellana, *FeynCalc 9.3: New Features and Improvements*, Comput. Phys. Commun. **256**, 107478 (2020), arXiv:2001.04407 [hep-ph].

Please have mercy.

Thank You

Thank you for your attention.

Questions are welcome.

Mass Parameters after Electroweak Symmetry Breaking

After EWSB, the scalar fields are written as

$$\Phi_1 = \begin{pmatrix} G^+ \\ (v + H_{\rm SM} + iG^0)/\sqrt{2} \end{pmatrix}, \qquad \Phi_2 = \begin{pmatrix} H^+ \\ (\rho + iA)/\sqrt{2} \end{pmatrix}, \qquad S = \rho_S .$$

The minimum condition $\partial V/\partial H_{\rm SM}|_0 = 0$ gives $m_{11}^2 = -\lambda_1 v^2/2$. The coefficient of $H_{\rm SM}^2/2$ is therefore

$$M_{H_{\rm SM}}^2 = \lambda_1 v^2 \qquad \Longrightarrow \qquad \lambda_1 = \frac{M_{H_{\rm SM}}^2}{v^2}.$$

Collecting the quadratic terms in $H^\pm$, A, ρ and ρ_S gives

$$M_{H^\pm}^2 = m_{22}^2 + \frac{\lambda_3}{2}v^2, \qquad M_A^2 = m_{22}^2 + \frac{\lambda_3 + \lambda_4 - \lambda_5}{2}v^2,$$

and

$$\mathcal{M}_{\rm even}^2 = \begin{pmatrix} m_S^2 + \frac{\lambda_7}{2}v^2 & \frac{\kappa_{12}}{2}v \\ \frac{\kappa_{12}}{2}v & m_{22}^2 + \frac{\lambda_{345}}{2}v^2 \end{pmatrix}_{(\rho_S,\rho)}, \qquad \lambda_{345} = \lambda_3 + \lambda_4 + \lambda_5 .$$

These relations follow by matching the quadratic part of the potential to $\frac{1}{2}M^2\varphi^2$ for a real field and $M^2 H^+ H^-$ for the charged field.

Source: Ref. [3], Eqs. (1)–(8).

Diagonalization Back

Diagonalization of the CP-Even Dark-Scalar Sector

The mass eigenstates are defined by

$$\begin{pmatrix} H_{D1} \\ H_{D2} \end{pmatrix} = R(\alpha) \begin{pmatrix} \rho_S \\ \rho \end{pmatrix}, \qquad R(\alpha) = \begin{pmatrix} \cos\alpha & \sin\alpha \\ -\sin\alpha & \cos\alpha \end{pmatrix}.$$

Since $R\mathcal{M}^2_{\text{even}}R^T = \text{diag}(M^2_{H_{D1}}, M^2_{H_{D2}})$, the mass matrix in the interaction basis can be reconstructed as

$$\mathcal{M}^2_{\text{even}} = R^T \begin{pmatrix} M^2_{H_{D1}} & 0 \\ 0 & M^2_{H_{D2}} \end{pmatrix} R = \begin{pmatrix} c_\alpha^2 M^2_{H_{D1}} + s_\alpha^2 M^2_{H_{D2}} & c_\alpha s_\alpha (M^2_{H_{D1}} - M^2_{H_{D2}}) \\ c_\alpha s_\alpha (M^2_{H_{D1}} - M^2_{H_{D2}}) & s_\alpha^2 M^2_{H_{D1}} + c_\alpha^2 M^2_{H_{D2}} \end{pmatrix},$$

where $c_\alpha = \cos\alpha$ and $s_\alpha = \sin\alpha$.
Matching the off-diagonal elements,

$$\frac{\kappa_{12} v}{2} = c_\alpha s_\alpha (M^2_{H_{D1}} - M^2_{H_{D2}}) = \frac{\sin(2\alpha)}{2}(M^2_{H_{D1}} - M^2_{H_{D2}}),$$

gives

$$\kappa_{12} = \frac{\sin(2\alpha)}{v}\left(M^2_{H_{D1}} - M^2_{H_{D2}}\right).$$

Matching the two diagonal elements gives

$$m_S^2 + \frac{\lambda_7}{2}v^2 = c_\alpha^2 M^2_{H_{D1}} + s_\alpha^2 M^2_{H_{D2}}, \qquad m_{22}^2 + \frac{\lambda_{345}}{2}v^2 = s_\alpha^2 M^2_{H_{D1}} + c_\alpha^2 M^2_{H_{D2}}.$$

Source: Ref. [3], Eqs. (7)–(10).

Previous
Inverted relations

Expressing Lagrangian Parameters in Terms of Physical Inputs

Define

$$\mathcal{M}_{\rho\rho}^2 \equiv \sin^2\alpha\, M_{H_{D1}}^2 + \cos^2\alpha\, M_{H_{D2}}^2.$$

From $\mathcal{M}_{\rho\rho}^2 = m_{22}^2 + \lambda_{345} v^2/2$ and $M_{H\pm}^2 = m_{22}^2 + \lambda_3 v^2/2$, subtracting the two equations gives

$$M_{H\pm}^2 = \mathcal{M}_{\rho\rho}^2 - \frac{\lambda_4+\lambda_5}{2} v^2.$$

Using $M_A^2 = m_{22}^2 + (\lambda_3+\lambda_4-\lambda_5)v^2/2$ and eliminating m_{22}^2, one finds

$$M_A^2 = \mathcal{M}_{\rho\rho}^2 - \lambda_5 v^2.$$

Finally, the original quadratic parameters follow directly from the charged and singlet diagonal mass terms:

$$m_{22}^2 = M_{H\pm}^2 - \frac{\lambda_3}{2} v^2, \qquad m_S^2 = \cos^2\alpha\, M_{H_{D1}}^2 + \sin^2\alpha\, M_{H_{D2}}^2 - \frac{\lambda_7}{2} v^2.$$

Therefore, the complete inverted relations are

$$\lambda_1 = \frac{M_{H_{\rm SM}}^2}{v^2}, \qquad \kappa_{12} = \frac{\sin(2\alpha)}{v}\left(M_{H_{D1}}^2 - M_{H_{D2}}^2\right),$$

$$M_{H\pm}^2 = \sin^2\alpha\, M_{H_{D1}}^2 + \cos^2\alpha\, M_{H_{D2}}^2 - \frac{\lambda_4+\lambda_5}{2} v^2, \qquad M_A^2 = \sin^2\alpha\, M_{H_{D1}}^2 + \cos^2\alpha\, M_{H_{D2}}^2 - \lambda_5 v^2,$$

$$m_{22}^2 = M_{H\pm}^2 - \frac{\lambda_3}{2} v^2, \qquad m_S^2 = \cos^2\alpha\, M_{H_{D1}}^2 + \sin^2\alpha\, M_{H_{D2}}^2 - \frac{\lambda_7}{2} v^2.$$

Source: Ref. [3], Eqs. (9)–(14).

Previous Back to mixing

Higgs–VLQ Cancellation Condition

For up-type quarks, the effective coupling is

$$c_u = \frac{m_u}{m_h^2}\left[\underbrace{\frac{\lambda_{H_{D1}H_{D1}H_{\rm SM}}}{v}}_{\text{Higgs contribution}} + \underbrace{\frac{m_h^2}{2m_{\rm VLQ}^2} Y_{\rm VLQ}^2 \sin^2\alpha}_{\text{VLQ contribution}}\right].$$

Defining

$$f_2 = f_1 + \frac{m_h^2}{2m_{\rm VLQ}^2} Y_{\rm VLQ}^2 \sin^2\alpha, \qquad f_1 = \frac{\lambda_{H_{D1}H_{D1}H_{\rm SM}}}{v},$$

destructive interference occurs when

$$f_2 \simeq 0.$$

Back

Higgs–VLQ Cancellation at the Quark Level

Denote the dark-matter particle by $D \equiv H_{D1}$ and the SM-like Higgs boson by $h \equiv H_{\mathrm{SM}}$. At small momentum transfer, the elastic scattering $Dq \to Dq$ is described by $\mathcal{L}_{\mathrm{eff}} = D^2 \sum_q c_q \bar{q} q$.

The Higgs-exchange contribution is $c_q^{(h)} = m_q \lambda_{DDh}/(v m_h^2)$, where $f_1 \equiv \lambda_{DDh}/v$ and

$$f_1 = -\lambda_7 \cos^2 \alpha - \frac{\kappa_{12}}{v} \cos\alpha \sin\alpha - \lambda_{345} \sin^2 \alpha, \qquad \lambda_{345} = \lambda_3 + \lambda_4 + \lambda_5.$$

For an up-type quark, the s/u-channel VLQ diagrams provide the additional contribution $c_u^{(T)} = m_u Y_{\mathrm{VLQ}}^2 \sin^2 \alpha/(2 m_{\mathrm{VLQ}}^2)$. Therefore, the total up-quark coefficient is

$$c_u = c_u^{(h)} + c_u^{(T)} = \frac{m_u}{m_h^2} \left[\underbrace{f_1}_{\text{Higgs}} + \underbrace{\frac{m_h^2}{2 m_{\mathrm{VLQ}}^2} Y_{\mathrm{VLQ}}^2 \sin^2 \alpha}_{\text{VLQ}} \right] \equiv \frac{m_u}{m_h^2} f_2.$$

Destructive interference occurs when the two terms have opposite signs and comparable magnitudes:

$$f_2 = f_1 + \frac{m_h^2}{2 m_{\mathrm{VLQ}}^2} Y_{\mathrm{VLQ}}^2 \sin^2 \alpha \simeq 0 \quad \Longleftrightarrow \quad \frac{\lambda_{DDh}}{v} \simeq -\frac{m_h^2}{2 m_{\mathrm{VLQ}}^2} Y_{\mathrm{VLQ}}^2 \sin^2 \alpha.$$

Since the VLQ term is non-negative, cancellation requires $f_1 < 0$ in the convention used in the proceeding. It is therefore not automatic, but occurs only in particular regions of parameter space.

Source: Ref. [3], Eqs. (18)–(23).

Nucleon level

Back

Cancellation at the Nucleon Level

The cancellation is incomplete at the nucleon level because the VLQ contributes only to the up-type-quark coefficient: $c_u = m_u f_2/m_h^2$, whereas $c_{d,s} = m_{d,s} f_1/m_h^2$. Define $A_u^{(N)} = \frac{1}{2} f_{Tu}^{(N)} + \frac{2}{27} f_{TG}^{(N)}$ and $A_d^{(N)} = \frac{1}{2}(f_{Td}^{(N)} + f_{Ts}^{(N)}) + \frac{1}{27} f_{TG}^{(N)}$. The spin-independent cross section is

$$\sigma_{\rm SI}^N = \frac{m_N^4}{(M_{D1} + m_N)^2 v^2 m_h^4 \pi} \left[\left(A_u^{(N)} \right)^2 |f_2|^2 + \left(A_d^{(N)} \right)^2 |f_1|^2 \right].$$

Hence, $f_2 \simeq 0$ suppresses the up-type contribution, but it does not generally imply $\sigma_{\rm SI}^N = 0$, because the down-type contribution proportional to $|f_1|^2$ remains. A very small cross section therefore requires both a cancellation in f_2 and a sufficiently small residual Higgs contribution f_1.
Writing $\Delta_{\rm VLQ} = m_h^2 Y_{\rm VLQ}^2 \sin^2\alpha/(2m_{\rm VLQ}^2) > 0$, the physical picture is simply

$$f_2 = f_1 + \Delta_{\rm VLQ} \simeq 0 \quad \Longrightarrow \quad \mathcal{M}_u^{(h)} + \mathcal{M}_u^{(T)} \simeq 0 \quad \Longrightarrow \quad \sigma_{\rm SI}^N \text{ is strongly suppressed.}$$

Thus, the Higgs and VLQ diagrams are genuine contributions of the model, but they cancel only when their amplitudes have opposite signs and nearly equal magnitudes. The proceeding demonstrates the possibility of such interference; it does not imply that every valid point lies exactly on the cancellation condition.

Source: Ref. [3], Eqs. (18)–(23).

Previous   Back to diagrams

Thermal Relic-Density Workflow

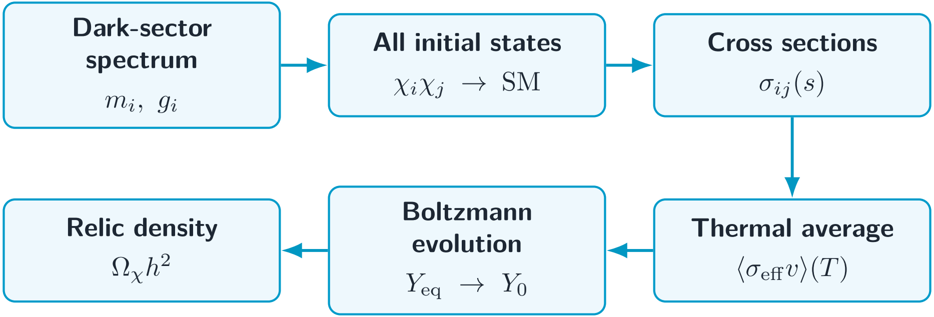

Gondolo–Gelmini provides the relativistic thermal average for annihilation, while Edsjö–Gondolo extends the same framework to coannihilating particles.

Step 1: From Amplitudes to Cross Sections

For each initial state,

$$\chi_i \chi_j \to X, \qquad \mathcal{M}_{ij\to X} \to |\mathcal{M}_{ij\to X}|^2.$$

Sum over all final states:

$$\sigma_{ij}(s) = \sum_X \sigma(\chi_i \chi_j \to X).$$

Define the invariant rate

$$W_{ij}(s) = 4p_{ij}\sqrt{s}\,\sigma_{ij}(s),$$

with

$$p_{ij} = \frac{\sqrt{[s-(m_i+m_j)^2][s-(m_i-m_j)^2]}}{2\sqrt{s}}.$$

The full s-dependence retains resonances, thresholds and interference effects.

J. Edsjö and P. Gondolo, Phys. Rev. D **56**, 1879 (1997).

Step 2: Thermal Average for One Species

For a dark-matter particle with mass m_χ,

$$\langle \sigma v \rangle (T) = \frac{\int_{4m_\chi^2}^{\infty} ds\, \sigma(s)(s - 4m_\chi^2)\sqrt{s}\, K_1(\sqrt{s}/T)}{8 m_\chi^4 T K_2^2(m_\chi/T)}.$$

Particle physics

$\sigma(s)$ contains masses, couplings, propagators, thresholds and resonances.

Thermal physics

K_1 and K_2 provide the relativistic Maxwell–Boltzmann weighting.

The relativistic thermal average requires only a one-dimensional integral over s.

P. Gondolo and G. Gelmini, Nucl. Phys. B **360**, 145 (1991).

Step 3: Determine the Freeze-Out Temperature

The annihilation rate is

$$\Gamma_{\rm ann}(T) = n_\chi^{\rm eq}(T)\,\langle\sigma v\rangle\,(T).$$

Thermal equilibrium

$$\Gamma_{\rm ann} \gg H \quad \Longrightarrow \quad n_\chi \simeq n_\chi^{\rm eq}.$$

Freeze-out

$$\Gamma_{\rm ann}(T_f) \simeq H(T_f).$$

Define

$$x = \frac{m_\chi}{T}, \qquad x_f = \frac{m_\chi}{T_f}, \qquad T_f = \frac{m_\chi}{x_f}.$$

T_f is determined self-consistently by the competition between annihilation and cosmic expansion.

P. Gondolo and G. Gelmini, Nucl. Phys. B **360**, 145 (1991).

Step 4: Evolve the Comoving Abundance

Define

$$Y = \frac{n_\chi}{s}, \qquad x = \frac{m_\chi}{T}.$$

The Boltzmann equation becomes

$$\frac{dY}{dx} = -\sqrt{\frac{\pi}{45G}}\,\frac{g_*^{1/2}(T)m_\chi}{x^2}\langle\sigma v\rangle\left(Y^2 - Y_{\rm eq}^2\right).$$

The cosmological factor is

$$g_*^{1/2} = \frac{h_{\rm eff}}{\sqrt{g_{\rm eff}}}\left(1 + \frac{T}{3h_{\rm eff}}\frac{dh_{\rm eff}}{dT}\right).$$

After integration,

$$Y_0 = Y(x \to \infty), \qquad \Omega_\chi h^2 \simeq 2.75 \times 10^8 \left(\frac{m_\chi}{\rm GeV}\right) Y_0.$$

P. Gondolo and G. Gelmini, Nucl. Phys. B **360**, 145 (1991).

Step 5: When Is Coannihilation Relevant?

Consider

$$\chi_1, \chi_2, \ldots, \chi_N, \qquad m_1 < m_2 < \cdots < m_N,$$

where χ_1 is the stable dark-matter particle.

Large mass splitting

$$m_i - m_1 \gg T_f$$

$$n_i^{\mathrm{eq}} \propto e^{-(m_i - m_1)/T} \ll n_1^{\mathrm{eq}}.$$

Coannihilation is negligible.

Small mass splitting

$$m_i - m_1 \lesssim T_f$$

The heavier particles remain populated, so

$$\chi_1 \chi_i \to \mathrm{SM}, \qquad \chi_i \chi_j \to \mathrm{SM}$$

can affect the relic abundance.

Coannihilation depends on both the mass splitting and the interaction strength of the heavier states.

J. Edsjö and P. Gondolo, Phys. Rev. D **56**, 1879 (1997).

Step 6: Define One Effective Boltzmann Equation

Define the total densities:

$$n = \sum_i n_i, \qquad n^{\text{eq}} = \sum_i n_i^{\text{eq}}.$$

Fast conversions maintain

$$\frac{n_i}{n} \simeq \frac{n_i^{\text{eq}}}{n^{\text{eq}}}.$$

The coupled system reduces to

$$\frac{dn}{dt} + 3Hn = -\langle \sigma_{\text{eff}} v \rangle \left(n^2 - n_{\text{eq}}^2 \right),$$

where

$$\langle \sigma_{\text{eff}} v \rangle = \sum_{i,j} \langle \sigma_{ij} v_{ij} \rangle \frac{n_i^{\text{eq}} n_j^{\text{eq}}}{(n^{\text{eq}})^2}.$$

The many-particle system behaves as one effective species while relative chemical equilibrium is maintained.

J. Edsjö and P. Gondolo, Phys. Rev. D **56**, 1879 (1997).

Step 7: Apply the Boltzmann Weights

Define

$$\Delta_i = \frac{m_i - m_1}{m_1}, \qquad x = \frac{m_1}{T}.$$

The effective number of degrees of freedom is

$$g_{\text{eff}}(x) = \sum_i g_i (1+\Delta_i)^{3/2} e^{-x\Delta_i}.$$

The equilibrium weight is

$$r_i(x) = \frac{g_i (1+\Delta_i)^{3/2} e^{-x\Delta_i}}{g_{\text{eff}}(x)}.$$

The effective thermal rate becomes

$$\langle \sigma_{\text{eff}} v \rangle = \sum_{i,j} r_i(x) r_j(x) \langle \sigma_{ij} v_{ij} \rangle .$$

A large σ_{ij} may still be irrelevant when

$$r_i r_j \ll 1.$$

Boltzmann suppression determines which annihilation and coannihilation channels actually control freeze-out.

J. Edsjö and P. Gondolo, Phys. Rev. D **56**, 1879 (1997).

Step 8: Effective Rate with Coannihilation

For each initial pair,

$$W_{ij}(s) = 4p_{ij}\sqrt{s}\,\sigma_{ij}(s),$$

where

$$p_{ij} = \frac{\sqrt{[s-(m_i+m_j)^2][s-(m_i-m_j)^2]}}{2\sqrt{s}}.$$

The effective invariant rate is

$$W_{\rm eff}(s) = \sum_{i,j} \frac{p_{ij}}{p_{11}} \frac{g_i g_j}{g_1^2} W_{ij}(s).$$

Define

$$p_{\rm eff} = p_{11}, \qquad s = 4(p_{\rm eff}^2 + m_1^2),$$

and

$$\mathcal{N}(T) = \sum_i \frac{g_i}{g_1} \frac{m_i^2}{m_1^2} K_2\left(\frac{m_i}{T}\right).$$

The thermal average becomes

$$\langle \sigma_{\rm eff} v \rangle = \frac{\int_0^\infty dp_{\rm eff}\, p_{\rm eff}^2 W_{\rm eff}(s) K_1\left(\frac{\sqrt{s}}{T}\right)}{m_1^4 T \mathcal{N}^2(T)}.$$

J. Edsjö and P. Gondolo, Phys. Rev. D **56**, 1879 (1997).

Complete Numerical Workflow

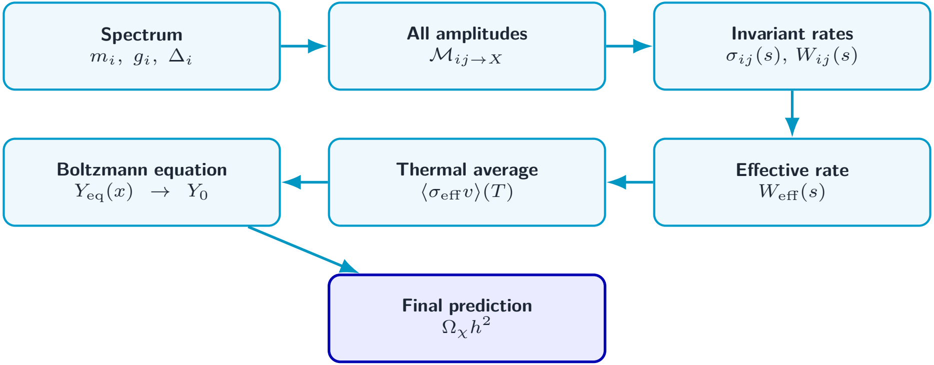

Essential consistency checks

No coannihilation $\Rightarrow W_{\rm eff} \to W_{11}$; thresholds begin at $\sqrt{s} = m_i + m_j$; large mass splittings $\Rightarrow$ Boltzmann suppression.